ELSEVIER

International Journal of Mass Spectrometry 192 (1999) 191–203

International Journal of Mass Spectrometry

Dynamics of chemical and charge transfer reactions of molecular dications: beam scattering and total cross section data on CF_2D^+ (CF_2H^+), CF_2^+, and CF^+ formations in CF_2^{2+} + $D_2(H_2)$ collisions

Z. Herman*, J. Žabka, Z. Dolejšek, M. Fárník[1]

V. Čermák Laboratory, J. Heyrovský Institute of Physical Chemistry, Academy of Sciences of the Czech Republic, Dolejškova 3, CZ-18223 Prague 8, Czech Republic

Received 12 January 1999; accepted 22 March 1999

Abstract

Dynamics of formation of the chemical rearrangement product CF_2D^+, the charge transfer product CF_2^+, and the dissociative products CF^+ and CFD^+ in collisions of the molecular dication CF_2^{++} with D_2 was investigated in crossed beam scattering experiments over the collision energy range 0.3–1.0 eV (center of mass). The scattering data show that coulomb repulsion between two singly charged products, CF_2^+ + D^+ and CF_2^+ + D_2^+, plays a dominant role in the nondissociative processes. A large fraction of the energy available (about 6 eV in the chemical reaction, about 4 eV in the charge transfer) goes into relative translational energy of the products. Relative total cross sections for formation of the nondissociative and dissociative products in collision of CF_2^{++} with D_2 and H_2 were determined over the collision energy range of 0.2–3.6 eV. The shape of the relative velocity dependence of the cross section for CF_2^+ formation can be described by a simple model based on the Landau-Zener formalism. The data suggest that the dissociative product CF^+ is formed prevailingly in a subsequent dissociation of the charge transfer product CF_2^+. A potential surface model is described which accounts for competition of various processes in dication–neutral collisions. (Int J Mass Spectrom 192 (1999) 191–203) © 1999 Elsevier Science B.V.

Keywords: Reaction dynamics; Elementary reactions of molecular dications; Ion scattering; Total cross sections

1. Introduction

Multiply charged ions are very energy-rich species, highly reactive in collisions with atoms and molecules. This is why they have attracted the increasing attention of experimentalists and theoreticians alike. Compared with the situation of a decade ago [1], much more information is available now, in particular on molecular doubly charged ions (molecular dications) [2]. Electronic states of diatomic or small polyatomic dications lie typically at energies above the asymptote for formation of the respective singly charged fragments. An energy barrier on the potential energy surface prevents them from dissociating and thus the observable molecular dications exist, in fact, in states metastable with respect to dissociation. Their lifetimes are often longer than about 10^{-5} s; therefore, molecular dications can be prepared and used as

* Corresponding author. E-mail: zdenek.herman@jh-inst.cas.cz

[1] Present address: J.I.L.A, University of Colorado, Boulder, CO 80308.

PII S1387-3806(99)00092-5

collision species. The energy barrier in many cases supports only the lowest vibrational states, and thus vibrational excitation is usually rather small.

In studies of collision processes of molecular dications, most often charge transfer processes of the type

$$A^{2+} + BC \rightarrow A^{+} + BC^{+} \quad (1)$$

(A, B, and C are atoms or groups of atoms) with atoms and molecules have been investigated, and large amounts of data have been obtained on the cross section and energy partitioning in the low collision energy region [2–4].

More recently, chemical (bond forming) reactions of doubly charged ions have been described in collisions of low energy ions with molecules. Chemical reactions of dications can basically be of two types: bond forming reactions between dications and neutrals where a doubly charged ion product and a neutral particle is formed, of the type

$$A^{2+} + BC \rightarrow AB^{2+} + C \quad (2)$$

or a reaction where two singly charged ions are formed as a result of a bond-rearrangement collision between a dication and a neutral,

$$A^{2+} + BC \rightarrow AB^{+} + C^{+} \quad (3)$$

The latter type is of a particular interest because of an expected high translational energy release due to coulomb repulsion between the products.

Early reports on chemical reactions of dications came from swarm experiments: their occurrence was briefly mentioned in flow tube studies of Ca^{2+} and Mg^{2+} interactions with simple molecules [5]. Several chemical reactions of transition metal doubly charged ions (Ti^{2+}, Nb^{2+}, Zr^{2+}, Ta^{2+}) in collisions with hydrogen and simple hydrocarbons, leading to both doubly and singly charged chemical products, have been reported [6–9]. More recently, bond-forming chemical reactions of molecular dications have been observed [10–13] where singly charged ions were formed in both nondissociative and dissociative chemical reactions.

In an earlier paper [11], the authors reported on a crossed beam scattering study of the nondissociative processes in collisions of CF_2^{2+} with D_2, namely of the chemical, bond-forming reaction

$$CF_2^{2+} + D_2 \rightarrow CF_2D^{+} + D^{+} \quad (4)$$

and the accompanying charge transfer process

$$CF_2^{2+} + D_2 \rightarrow CF_2^{+} + D_2^{+} \quad (5)$$

The results at the relative collision energy of 0.6 eV showed that the type of scattering of ion products of reactions (4) and (5) was rather similar and governed by coulomb repulsion between the products. The relative translational energy release represented in both cases a larger fraction of the reaction exoergicity, the peak value being about 6 and 4 eV in reactions (4) and (5), respectively. We formulated a simple model for the chemical reactions of dications based on crossing of the potential energy surfaces of the reactant dication system with coulomb-repulsion surfaces of the cation products both in the reactant and the product valley.

In this article, we report further scattering data on reactions (4) and (5) at relative collision energies of 0.3 and 1.0 eV, results of measurements of total cross sections of the reactions with D_2 and H_2, data on the dissociation product CF^{+}, and we extend the discussion of the above mentioned model.

2. Experimental

The experiments were carried out on the crossed beam apparatus EVA II (Fig. 1). The CF_2^{2+} dications were produced by impact of 130 eV electrons on CF_4 in a low pressure ion source. Ions were extracted, mass analyzed, and decelerated by a multielement lens to the required laboratory energy. The CF_2^{2+} beam was crossed at right angles with a beam of D_2 (H_2) molecules emerging from a multichannel jet. The ion beam had an angular and energy spread of 1° and 0.3 eV [full width at half maximum (FWHM)], respectively; the collimated neutral beam had an angular spread of 6° (FWHM) and thermal energy distribution at 300 K. Reactant and product ions passed through a detection slit (2.5 cm from the scattering center) into a stopping potential energy analyzer, they were then accelerated and focused into

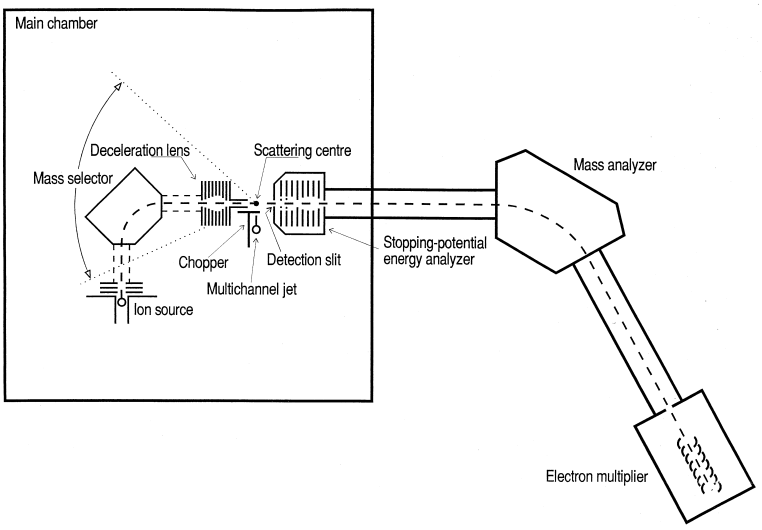

Fig. 1. Schematics of the crossed-beam scattering apparatus EVA II.

the detection mass spectrometer, mass analyzed, and detected with the use of a dynode electron multiplier. Angular distributions were obtained by rotating the two beams about the scattering center. Modulation of the neutral beam and phase-sensitive detection of the ion products was used to remove the background scattering effects.

Laboratory angular distributions and energy profiles recorded at six to ten laboratory scattering angles were used to construct scattering diagrams of the products CF_2D^+, CF_2^+, and CF^+ showing contours of the Cartesian probability distribution [14]. Center-of-mass (c.m.) angular distributions (relative differential cross sections) and relative translational energy distributions of the products were then obtained in the usual way [14].

In the measurements of the total cross sections, the dependence on the collision energy for the ratio of the intensities product ion/reactant ion, $I_{P,m}/I_{R,m}$, was measured at the ion angular maximum, at a constant pressure of the neutral reactant (D_2 or H_2). The relative total cross section σ_{rel} was then determined as

$$\sigma_{\text{rel}} = I_{P,m}/I_{R,m} \int I_P(\Theta) d\Theta / I_{P,m} \qquad (6)$$

The correction factor $\int I_P(\Theta) d\Theta / I_{P,m}$ is a normalized integral over the laboratory angular distribution of the product. This is, of course, only an approximate correction, as it assumes that the product ions have all the same velocity at a particular collision energy. However, because the scattering diagrams of the products are rather similar, this method turned out to be more accurate than integrating the (absolute) Cartesian probability distribution over the scattering diagram. Anyway, the correction factor played only a minor role. The scatter in the measured data (Figs. 7 and 8) comes mainly from difficulties of locking in exactly the phase of the product ion signal when determining the ratio of the product ion intensity (modulated ac signal) to the reactant ion intensity (dc signal). The values of the relative total cross sections in Figs. 7 and 8 are mutually in scale.

3. Results and discussion

3.1. Scattering data on CF_2D^+ and CF_2^+

Scattering contour diagrams of ion products CF_2D^+ and CF_2^+ formed in reactions (4) and (5) at relative collision energies 0.3 and 1.0 eV, are shown in Figs. 2 and 3, respectively. The horizontal line denotes the direction of the relative velocity vector (CF_2^{2+} approaching from the left), c.m. shows the

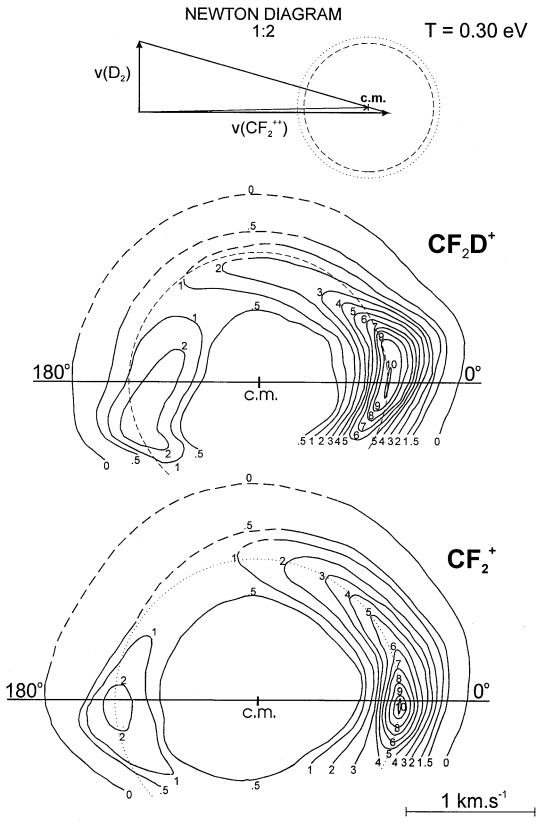

Fig. 2. Contour scattering diagrams of products CF_2D^+ and CF_2^+ from reactions (4) and (5) at collision energy $T = 0.3$ eV (c.m.). The horizontal line shows the direction of the relative velocity vector, c.m. marks the position of the tip of the center-of-mass velocity vector. Upper panel shows the respective Newton diagram (scale 1:2); the circles in it correspond to the circles drawn through the angular maxima in the scattering diagrams of CF_2D^+ (dashed) and CF_2^+ (dotted).

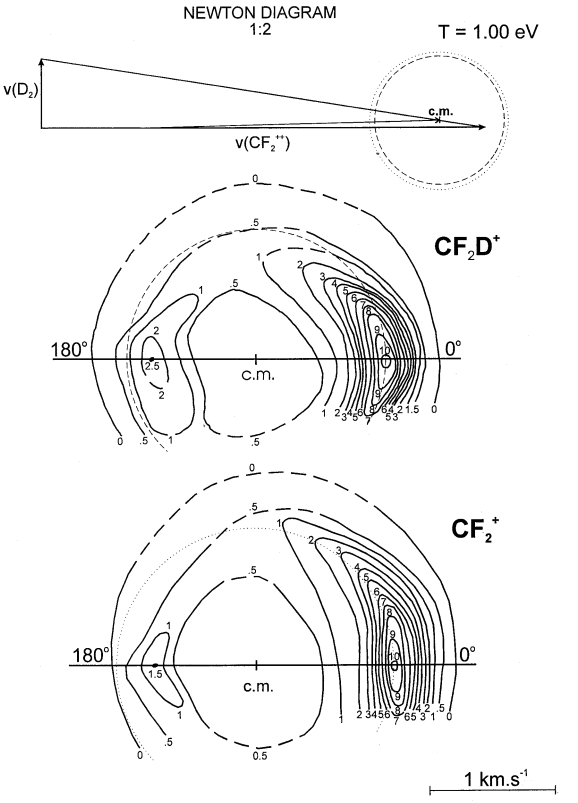

Fig. 3. Contour scattering diagrams of products CF_2D^+ and CF_2^+ from reactions (4) and (5) at collision energy $T = 1.0$ eV (c.m.). Further details same as in Fig. 2.

position of the tip of the velocity vector of the center of mass. The top panels give the respective Newton diagrams.

All diagrams are rather similar: they show that the measured ion product is scattered prevailingly in the forward direction (with respect to the incoming dication), the backward scattering is much weaker and somewhat more pronounced in the case of the CF_2D^+ product. The distance between the c.m. and the maximum contour is about equal at both collision energies. This indicates that the main factor influencing the translational energy release is the coulomb repulsion between the products, the effect of the relative translational energy of reactants is rather small. The data in Fig. 2 clearly show some broadening, reflecting an increased effect of velocity spreads in the beams on the scattering at this low collision energy. The scattering data published earlier [11] are in agreement with the results presented here.

Fig. 4 shows the summary of the data on c.m. angular distributions, $P(\vartheta)$ versus ϑ, including the earlier published data [11] at the collision energy of 0.6 eV. The data are in general agreement exhibiting strong forward scattering of the heavy ion product, a small portion of large angle scattering (about 10%–15%), and a slightly increased probability of scattering in the backward direction. In case of chemical reaction (4) this backward scattering is equal (see Fig. 2) or larger (see Figs. 3 and 4) than the relevant

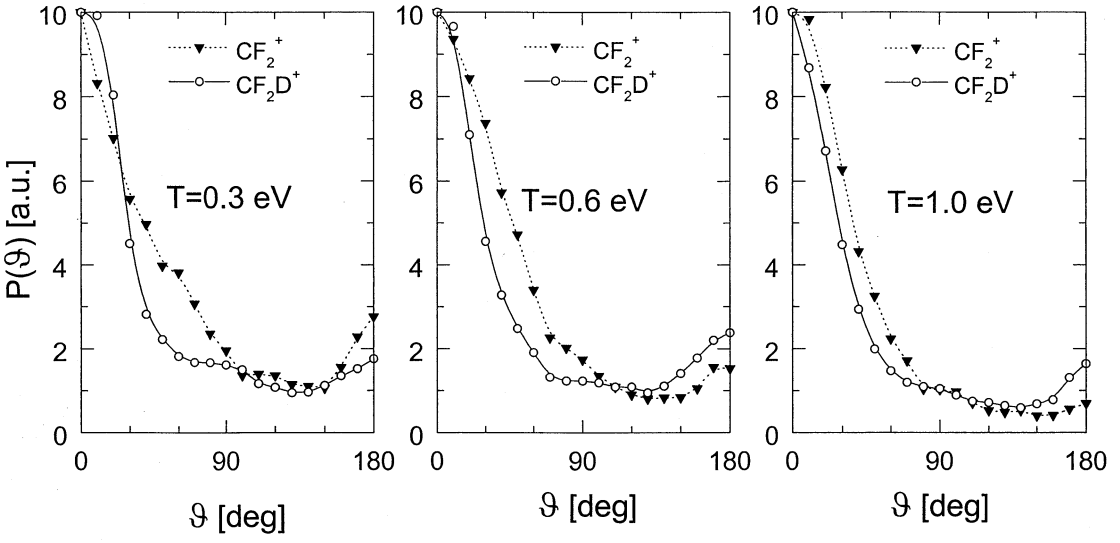

Fig. 4. Relative differential cross sections (c.m. angular distributions), $P(\vartheta)$ vs. ϑ, of CF_2D^+ (solid line) and CF_2^+ (dotted) from reactions (4) and (5), respectively, at the collision energies of 0.3, 0.6, [11], and 1.0 eV.

scattering in charge transfer process (5). This may indicate that a fraction of trajectories of the "snarled" type (sticky collisions implying formation of an intermediate) contributes to the formation of the chemical rearrangement product CF_2D^+.

Fig. 5 summarizes data on the overall product relative translational energy distributions, $P(T')$ versus T', derived from the scattering diagrams. Vertical arrows indicate maximum energy available in reactions (4) and (5). The energetics of the system was derived from thermochemical data [15], from the photoelectron spectroscopy of CF_2 [16], and with the use of a recent value of $\Delta H_f(CF_2^{2+}) = 687 \pm 5$ kcal/mol* [17]; it is shown in an energy diagram in Fig. 6. The exoergicities of reactions (4) and (5) are 7.60 and 5.04 eV, respectively. The $P(T')$ curves show a tendency of extending beyond the maximum energy available in the process. This could be due to participation in the reaction of an excited state of the reactant dication lying about 4 eV above the ground state; the existence of such a state was postulated earlier [18] to explain the occurrence of several dissociative charge transfer processes in collisions with rare gases, and it was also confirmed by recent translational-energy-spectroscopy studies of charge transfer between CF_2^{++} and Ne [19]. However, the tailing seems to depend on the collision energy being least pronounced at the highest collision energy of 1 eV, where the effects of velocity spreads in the reactant beams is smallest. Thus it is quite likely that the tailing is due only to an inaccuracy of the experiments: the velocity spreads in the reactant beams lead to a broadening of the scattering diagrams which is then accented by unfavorable kinematics (recoil of the measured heavy ion on a light second reaction product) in the $P(T')$ calculation.

The $P(T')$ curves in Fig. 5 show that—of the total energy available in chemical reaction (4)—about 5.5–6.5 eV appear as relative translational energy of the products, a huge amount for a chemical reaction, and about 1–2 eV as internal excitation (vibrational and rotational) of the molecular product. In charge transfer reaction (5), the distribution peaks at 4.1, 4.5, and 4.4 eV for the collision energies of 0.3, 0.6, and 1.0 eV, respectively. This means that the fraction of

*This value is substantially smaller than the value derived from appearance potential measurements (767 kcal/mol) and used in [11].

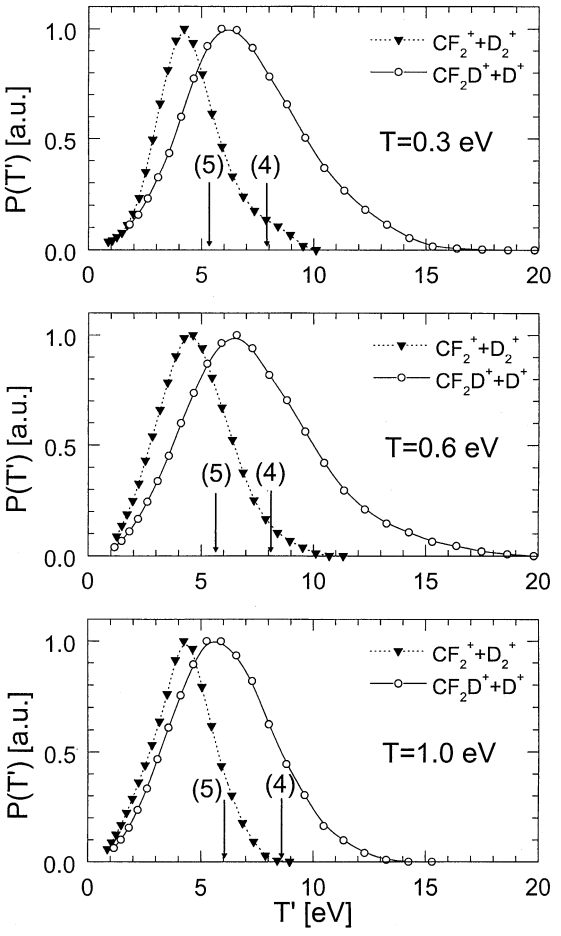

Fig. 5. Relative translational energy distributions, $P(T')$ vs. T', of products of reactions (4) and (5), at the collision energies of 0.3, 0.6, [11], and 1.0 eV; arrows mark the maximum energy available in reactions (4) and (5).

energy deposited as internal energy of the charge transfer products CF_2^+ and D_2^+ (as derived from the distribution maxima) is 1.24, 1.14, and 1.64 eV, for the three collision energies, respectively. The average from these three values is 1.34 eV. This result can be compared with the translational energy release in the charge transfer

$$CF_2^{2+} + Ar \rightarrow CF_2^+ + Ar^+ \quad (7)$$

reported earlier [19]. Reaction (7) differs from reaction (5) slightly in exoergicity (4.71 eV versus 5.04 eV, respectively) and in that the two spin-orbit states

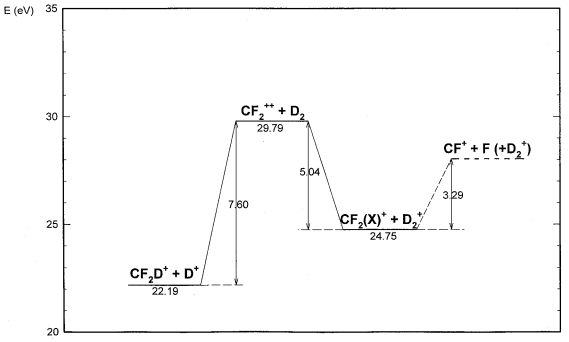

Fig. 6. Energetics (in electron volts) of processes (4), (5), and of CF^+ ($+F + D_2^+$) formation in the system $CF_2^{++} + D_2$.

of Ar^+ may be populated in reaction (6). In reaction (7) about 1.1 eV was found to go into internal excitation of the molecular product CF_2^+. Comparing this value with the average value of estimated internal energy in the charge transfer with molecular D_2, 1.34 eV, suggests that—assuming that the internal energy deposited in CF_2^+ is in both cases the same—a part of the energy available, about 0.25 eV, is deposited as internal energy of the other molecular ion product, D_2^+. This corresponds to most probable vibrational excitation of D_2^+ to ($v = 1,2$). This approximate result is in general agreement with the earlier findings [20] that in charge transfer processes of this type vibrational excitation of the molecular products is approximately described by the Franck-Condon overlap of the respective reactant and product states.

3.2. Total cross sections

Results on measurements of the total cross sections of reactions (4) and (5) and of the analogous reactions with H_2 are summarized in Fig. 7. The data are plotted as a function of the reactant relative velocity, v_{rel}. In this representation the charge transfer data, reaction (5), for both D_2 and H_2 collapse, within the accuracy of the measurements, to a single line descending steeply with decreasing relative velocity. On the other hand, total cross sections for the chemical reactions slowly increase with decreasing relative velocity, pass through a maximum at about $v_{rel} = 6.5$ km/s for both D_2 and H_2, and then they seem to decrease below

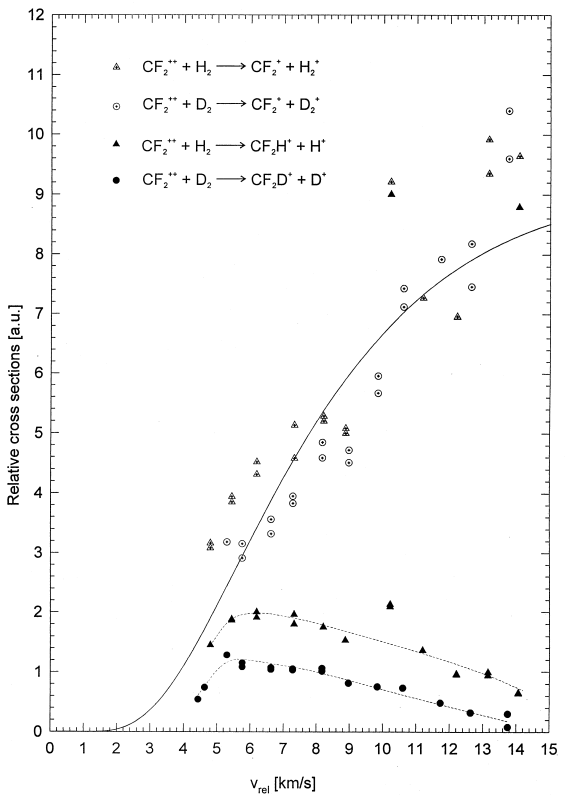

Fig. 7. Relative total cross sections of nondissociative chemical and charge transfer reactions in collisions of CF_2^{++} with D_2 and H_2 as a function of the relative velocity of the reactants, v_{rel}. The solid line is a result of Landau-Zener calculations for the charge transfer process (see text). The dashed lines only connect experimental points for a better orientation.

v_{rel} = 6 km/s. They show an isotope effect favoring the reaction with H_2 about 1.5–2 times in comparison with the reaction in which D_2 is the reaction partner. In the maximum at v_{rel} = 6 km/s the total cross section for the chemical reaction is about 60% (H_2) and 30% (D_2) of the cross section for the charge transfer reaction.

The decrease of the charge transfer total cross section with decreasing relative velocity can be rationalized in terms of the Landau-Zener model (also see discussion in Sec. 3.4). In an application of this formalism [21], the probability p of the electron remaining on the same diabatic curve in a single passage through the crossing at R_C can be written as

$$p = \exp\left(- \frac{\pi |H_{12}|^2}{2h|V_1 - V_2|v_R} \right) \quad (8)$$

where H_{12} is the coupling element which can be estimated by the Olson's method [21,22], $V_1 = -Z^2e^2\alpha/r^4$ is the ion-induced dipole potential between the reactants, and $V_2 = e^2/r - \Delta E$ is the coulomb repulsion potential between the charge transfer products. The radial velocity v_R is related to the relative velocity v_{rel} by

$$v_R = v_{rel}\,(1 - b^2/R_C^2)^{1/2} \quad (9)$$

The most probable value of the radial velocity was estimated by considering how the radial velocity varied when the relative velocity was calculated as a function of the impact parameter for $0 \leq b \leq b_{max}$; $v_R = 0.7\ v_{rel}$. The plot of the transition probability $P = p\ (1 - p)$ dependent on the relative velocity is shown in Fig. 7 as a dotted line. It can be seen that this simple model accounts reasonably well for the shape of the dependence of the charge transfer integral cross section on the relative velocity. We are aware that we apply here the Landau-Zener formalism to crossings of potential energy surfaces (rather than curves) and without an analysis of the possible molecular terms which arise from the interaction. However, we find it worth mentioning that even this simple interpretation leads to satisfactory results.

3.3. Formation of the product CF^+

Measurements on the integral cross section and scattering of the ion product CF^+ provide insight into the mechanism of formation of this dissociative product.

Fig. 8 shows the relative total cross section for the formation of CF^+ in $CF_2^{++} + D_2$ and $CF_2^{++} + H_2$ collisions in dependence on the relative velocity. The ordinate scale can be compared with the ordinate scale in Fig. 7. The data show a steep decrease of the cross section with decreasing relative velocity which strongly resembles the decrease of the integral cross section for charge transfer process (5). The ratio of the two cross sections, $\sigma(CF^+)/\sigma(CF_2^+)$, is about 0.25. This suggests that the formation of CF^+ is connected

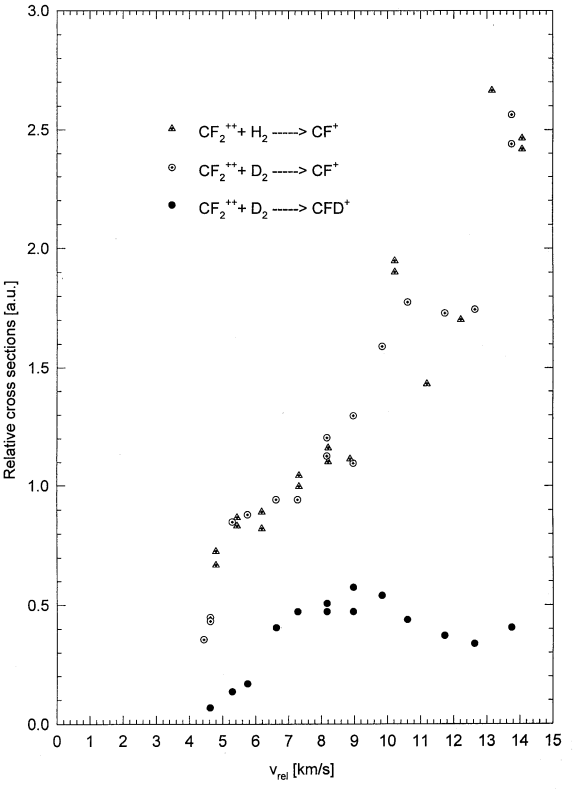

Fig. 8. Relative total cross sections for CF^+ and CFD^+ formation in collisions of CF_2^{++} with D_2 and H_2 as a function of the relative velocity of reactants, v_{rel}. The ordinate scale can be compared with that in Fig. 7.

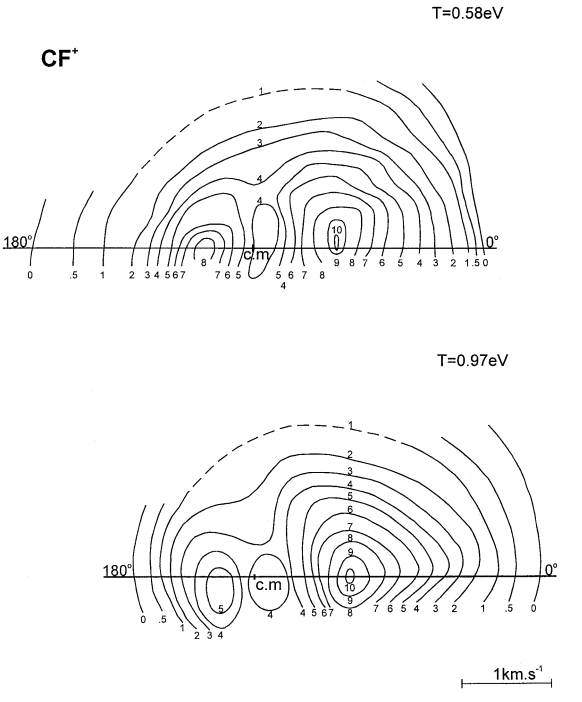

Fig. 9. Contour scattering diagrams of CF^+ formed in CF_2^{++} + D_2 at the collision energy of 0.58 and 0.97 eV, respectively. Details same as in Fig. 2.

with the charge transfer process and that the main channel of this dissociative product formation is subsequent dissociation of a part of CF_2^+ formed in charge transfer reaction (5).

Scattering data on CF^+ support this conclusion: in Fig. 9(a) and (b) the scattering diagrams of CF^+ formed in the CF_2^{++} + D_2 collisions at 0.58 and 0.98 eV are presented. The scattering diagrams resemble at first sight somewhat blurred scattering diagrams of CF_2^+ from reaction (5) [see [11] and Fig. 3(b)]. However, the product peaks at a smaller velocity in the forward direction and the backward scattering is considerably stronger and more inelastic, in comparison with the diagrams for the product CF_2^+.

Fig. 10(a) and (b) summarizes further information derived from the scattering diagrams in Fig. 9(a) and (b) the c.m. angular distributions and the product relative translational energy distributions, for the two collision energies of 0.58 and 0.98 eV, respectively. The $P(T')$ curves in Fig. 10 are plotted in dependence on two different product relative translational energy scales: T'(CF–FD_2) is the relative energy of CF^+ with respect to $(D_2 + F)^+$, the T' scale is CF_2^+ (CF^+ + F) with respect to D_2^+. Thus the latter shows the position of CF^+ formed by dissociation from CF_2^+ after its interaction with D_2^+ and (assuming little energy release between the dissociation product pair CF^+ + F) it approximately traces the position of CF_2^+ which dissociated. Fig. 11 then compares the translational energy distribution of the charge transfer products of reaction (5) from Fig. 5 with those of CF^+ from Fig. 10, plotted as a function of T' (CF_2^+ − D_2^+).

The plots in Fig. 11 suggest what characterizes the CF_2^+ ions which dissociates to CF^+. The curve for CF^+ peaks at 2.9–3.2 eV below the maximum energy available in charge transfer process (5), i.e. close to

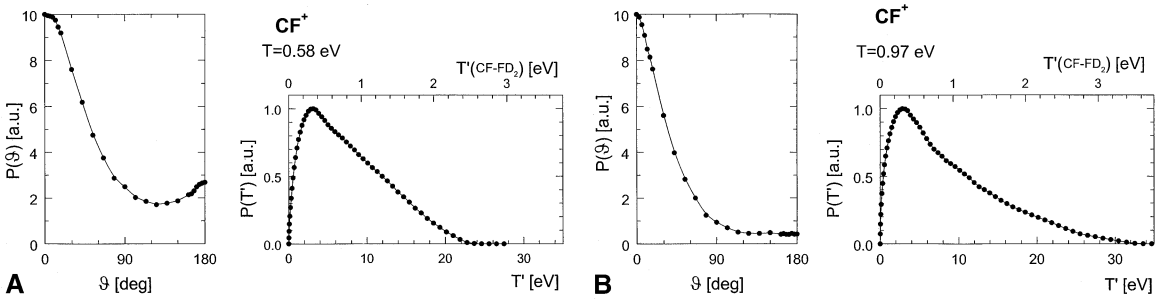

Fig. 10. Relative differential cross sections (c.m. angular distributions), $P(\vartheta)$ vs. ϑ, and product relative translational energy distributions, $P(T')$ vs. T', of CF^+ formed in $CF_2^{++} + D_2$ collisions at the collision energy of (a) 0.58 eV and (b) 0.97 eV. Note that the relative translational energy T' refers to product pair $CF_2^+ + D_2^+$ (see text), the relative translational energy CF^+ with respect to $(F–D_2^+)$, $T'(CF–FD_2)$, is shown in the upper scale.

the energy threshold for dissociation of CF_2^+ to CF^+ (energy diagram in Fig. 5). Besides that, the low energy parts of the plots in Fig. 11 indicate that the CF^+ is preferentially formed from CF_2^+ of small translational energy, i.e. of high internal excitation. The high energy part of the CF^+ curves in Fig. 11 has little meaning, because the procedure of calculating $P(T')$ from the scattering diagram exaggerates the blurring effect of the energy release in the dissociation process to $CF^+ + F$ and this results in excessive tailing of the curve to unrealistic high energies.

Thus it seems plausible to conclude that CF^+ formed in $CF_2^+ + D_2$ collisions comes prevailingly from a subsequent dissociation to $CF^+ + F$ of the charge transfer product CF_2^+ of low translational energy and hence high internal excitation.

For completeness, data on the relative total cross section of the product CFD^+ are given in Fig. 8, too. The shape of the relative velocity dependence is similar to that for the reaction product CF_2D and thus this appears to be the mostly likely precursor of CFD^+. Unfortunately, scattering information could not be obtained, because of a very low intensity of the CFD^+ ion signal.

3.4. Discussion of the potential surface model

In earlier papers [3,11] a simple potential surface model which accounts for the competition of charge transfer (1) and chemical reactions (2) and (3) in collisions of dications with neutral molecules is introduced. Three types of potential energy surfaces are involved. (1) A potential energy surface of the dication $A^{2+} + BC$ which continues into the chemical product valley as the dication system $AB^{2+} + C$; (2) coulomb repulsion surfaces in the reactant valley leading to charge transfer products $A^+ + BC^+$ (and possibly to further dissociative charge transfer products); (3) coulomb repulsive surfaces in the product valley leading to chemical rearrangement singly charged products $AB^+ + C^+$ (and possibly to the related dissociative products).

The existence or non-existence of crossings between the dication surface and coulomb repulsive surfaces at different interparticle separation influences the outcome of a dication–neutral collision and represents an application of the “reaction window” concept to chemically reactive systems. The situation is schematically shown in Fig. 12 as an energy profile along the reaction coordinate from the reactant to the product valley. The system approaches along the slightly attractive (ion-induced dipole) term marked $A^{2+} + BC$. In general, several possible cases of crossings between mutually interacting terms should be considered (Fig. 12).

(1) Crossings at large interparticle (A–BC) separations in the reactant valley, R1: small exoergicities of reaction (1), $\Delta E(1) < 2$ eV (e.g. a low value of the ionization energy $IE(A^+ \rightarrow A^{2+})$ in comparison with $IE(BC \rightarrow BC^+)$, excited states of A^+* and/or BC^+*), lead to a diabatic character

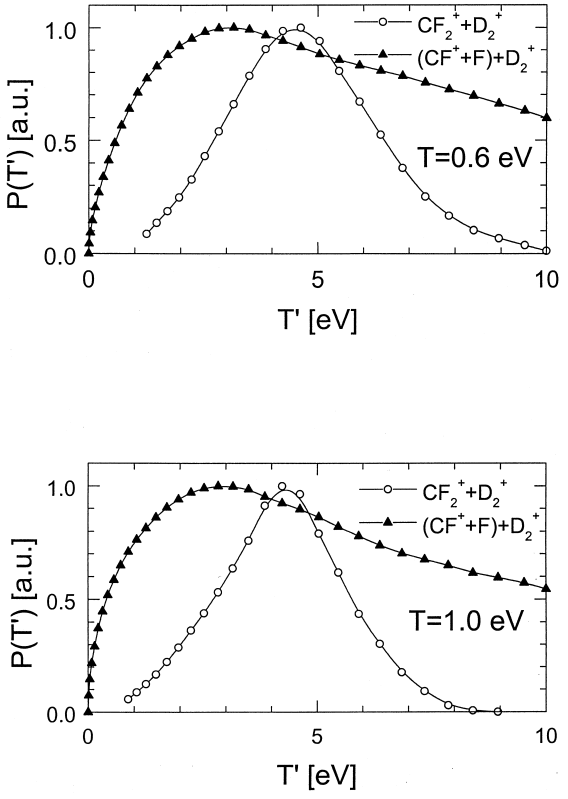

Fig. 11. Comparison of the relative translational energy distributions of $CF_2^+ + D_2^+$ from reaction (5) (Fig. 5) with those of $(CF^+ + F) + D_2^+$ (Fig. 10); T' refers to the product pair $CF_2^+ + D_2^+$.

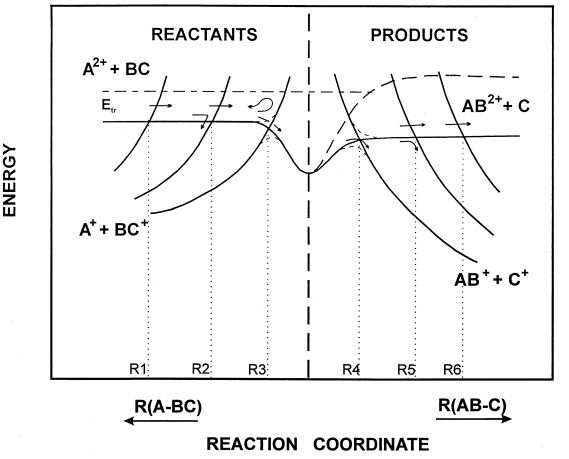

Fig. 12. Schematics of the potential energy surfaces and their possible crossing for dication-neutral reactions. For details of the model see text.

of the crossing, the single-passage probability of remaining on the same potential energy surface, $p_1 \approx 1$, and the system tends to continue as $AB^{2+} + C$ to smaller interparticle separations.

(2) Crossings at intermediate interparticle separations, R2: exoergicities $\Delta E(1)$ of about 3–5 eV result in a finite transition probability in the vicinity of the crossing, $0 < p_1 < 1$, to the products of the charge transfer $AB^+ + C^+$.

(3) Crossings at small interparticle separations, R3: large exoergicities, $\Delta E(1) > 6$ eV [large values of IE $(A^+ \rightarrow A^{2+})$], small IE$(BC \rightarrow BC^+)$ lead to large adiabatic splitting at R3, $p_1 \approx 0$, and the system is reflected with a high probability back towards the reactants.

(4) Crossings at small interparticle separations in the valley of products, R4: large exoergicity of the chemical rearrangement process, $\Delta E(2) > 6$ eV [small ionization energy IE$(C \rightarrow C^+)$], large second ionization energy IE$(AB^+ \rightarrow AB^{2+})$ leads to a large adiabatic splitting at R4 ($p_2 \approx 0$) which favors the way from small interparticle separations towards the chemical rearrangements products $AB^+ + C^+$.

(5) Crossings at intermediate separation in the product valley, R5: exoergicities of the chemical rearrangement process (2), $\Delta E(2)$ of about 3–5 eV, make $0 < p_2 < 1$, and both products $AB^+ + C^+$ and $AB^{2+} + C$ may be formed.

(6) Crossings at large interparticle separations in the product valley, R6: small exoergicities of reaction (2), $\Delta E(2) < 2$ eV lead to a diabatic crossing and allows for the formation of the dication rearrangements products $AB^{2+} + C$.

This simple model suggests explanations for some of the features of dication reactions so far observed. Also, it appears to be useful in describing the chemical reactivity of doubly charged fullerene ions [23] and it may be of use in a better understanding of some aspects of unimolecular decompositions of polyatomic multicharged ions. First of all, it indicates why chemical reactions of dications tend to occur much

less frequently than charge transfer processes [reaction (1)]: the colliding reactants have to pass through the charge transfer crossings in the reactant valley to reach small interparticle separations in order to react chemically, and the number of systems which succeed in it may be considerably reduced. In addition, a large adiabatic splitting at R3 may reflect the systems back into the reactant valley and effectively prevent formation of chemical rearrangement products. However, when this is not the case, chemical reactions may be easily observed; the reaction probability depends on the behavior of the system at small inter-particle separations. This is presumably why several transition metal ions (Ti^{2+}, Nb^{2+}, Zr^{2+}) turned out to react effectively to form chemical rearrangement products [6–9] in reactions (2) and (3). The difference of the first and second ionization energy of the metal atom Me, IE($Me^+ \rightarrow Me^{2+}$), is about 12 eV for these ions and this makes a charge transfer reaction with hydrogen or methane (and even ethane) either endoergic or only slightly exoergic. Thus the reactant valley is relatively free of effective crossings to charge transfer products and the colliding systems may reach the small interparticle separations which make chemical reactions (2) and (3) possible.

Formation of the chemical rearrangement dication products, AB^{2+} + C, is even more difficult, as the systems have to pass through the possible crossings with coulomb repulsion surfaces in the product valley which lead to $AB^+ + C^+$. Also, endoergicity of reaction (3) may be an effective block of forming AB^{2+} + C (dashed line in Fig. 12). This appears to be the case in the formation of ArN^{2+} in $Ar^{2+} + N_2$ collisions, described recently [24]: the reaction with the ground state $Ar^{2+}(^3P)$ is probably endoergic and the state becomes reactive only at fairly high collision energies.

The behavior of the system at small interparticle separations (Fig. 12 between R3 and R4) depends on the stability of the collision species ABC^{2+}. For relatively flat surfaces the system may be expected to go in a single-passage type trajectory into the product valley. If, however, ABC^{2+} is appreciably stable with respect to dissociation to both A^{2+} + BC and AB^{2+} + C and the surface exhibits a well, an intermediate complex may be formed with a mean lifetime of many rotations. The prevailing type of the collision mechanism should be reflected in the angular scattering (differential cross section).

Reactions (1) and (2) are strongly exoergic processes and product dissociation channels often lie below the energy of both A^{2+} + BC and AB^{2+} + C. Therefore, dissociative processes and formation of dissociation products is very frequent [9,16]. In fact, in many cases the nondissociative products of reactions (1) and (2) are—unlike in the system CF_2^{++} + D_2—very minor products or not observable at all. The mechanism of formation of the dissociative products may be in principle more complicated than the formation of CF^+ as analyzed here, and it should be investigated for a variety of systems before any general conclusions are made.

Finally, we apply the described potential surface model to the investigated system CF_2^{++} + D_2. The most important approach of the reactants is on a singlet potential energy surface of the ground state $CF_2^{++}(^1\Sigma^+)$ and $D_2(^1\Sigma_g^+)$. In the reactant valley there is an effective crossing with the family of the coulomb repulsive potential energy surfaces correlating with the charge transfer products $CF_2^+(X,\ 6a_1)$ [15] + $D_2^+(^2\Sigma^+)$ of an exoergicity of 5.08 eV in the vicinity of $R_1 \approx 3.2$ Å. Other, less exoergic channels correlating with excited $CF_2^+(A,\ 4b_2)$ and $CF_2^+(B,\ 1a_2)$ [15] and D_2^+ have exoergicities of 0.8 and 0.2 eV, respectively, and possible transitions at crossings at 18 Å and >70 Å do not have to be considered. Also, the reactants channel involving excited CF_2^{++} can be neglected in our considerations as its contribution to the product formation is presumably small (see also Sec. 3.1). The Landau-Zener probability (applied to molecular systems) for the passage through the region at R_1, p_1, was calculated as described in Sec. 3.2 and the probability for forming the charge transfer products as a function if the relative velocity was determined and compared with experimental results in Fig. 7. The probability of the system remaining on the dication CF_2^{++}–D_2 surface after the passage through R_1 to smaller interparticle separations is p_1. Preliminary calculations of the dication hypersurface [25] indicate that the collision species $CF_2D_2^{++}$ is more

stable with respect to the reactants by several eV and thus there exists a well at small interparticle separations. An indication of possible contribution of "snarled" trajectories from the increased backward scattering in CF_2D^+ c.m. angular distributions is consistent with the existence of such a well. In the valley of products the dication surface along the reaction coordinate probably rises toward the dication products CF_2D^{++} + D. Little is known about the dication CF_2D^{++}, but a rough estimation of its ionization energy from the radical neutral precursor using the Eland's approximate method [26] suggests that the products CF_2D^{++} + D may lie about 2–3 eV above the reactants CF_2^{++} − D_2. However, at rather small interparticle separations there is a crossing leading to a pair of singly charged chemical products CF_2D^+ + D^+. (exoergicity 7.6 eV, $R_2 \approx 1.8$ Å). An estimation of the formal Landau-Zener probability of a single-passage through this region suggests that $p_2 \approx 0$, indicating a substantial adiabatic splitting of the surfaces. However, any more conclusions about the reactive process, the reaction probability, the transition probability in the vicinity of the crossing, its influence on the cross section of reaction (4), etc. are impossible without more information on the potential energy surfaces in this region.

4. Conclusions

(1) Formation of CF_2D^+ (nondissociative chemical rearrangement reaction), CF_2^+ (nondissociative charge transfer), CF^+, and CFD^+ (dissociative processes), and the respective isotopic variants was investigated in dication–neutral CF_2^{++} + $D_2(H_2)$ collisions over the collision energy range 0.2–3.6 eV (c.m.). Crossed-beam scattering experiments were carried out to obtain scattering diagrams, differential cross sections, and product relative translational energy distributions for CF_2D^+, CF_2^+, and CF^+ (collision energies 0.3–1.0 eV). Relative total cross sections were obtained for all products over the collision energy range 0.2–3.6 eV (c.m.).

(2) The dynamics of CF_2D^+ and CF_2^+ formation, respectively, is dominated by coulomb repulsion between two singly charged products formed. Differential cross sections are characterized by a strong forward peak of the heavy molecular product and a smaller (10%–20%) fraction of sideways and backward scattering; a somewhat larger backward scattering of CF_2D^+ (in comparison with CF_2^+) may indicate a contribution of snarled trajectories in the chemical rearrangement product formation. Product relative translational energy distributions show that the most probable partitioning of energy in the chemical reaction is about 6 eV into relative translational energy of the products (a huge amount for a chemical process) and about 1.5 eV into the internal energy of the molecular product, in the charge transfer about 4 eV into relative translation and about 1.3 eV into internal excitation of the product ions.

(3) Relative total cross section for the formation of CF_2^+ decrease with decreasing collision energy and its dependence on the relative velocity of the reactants can be described by the Landau-Zener model. Relative total cross section for the chemical product formation represents about 0.6 (CF_2H^+) and 0.4 (CF_2D^+) of the value for CF_2^+ formation at low collision energies and decreases with increasing collision energy. There is and isotope effect of 1.5–2.0 favoring formation of CF_2H^+ over CF_2D^+.

(4) Total and differential cross section measurements of CF^+ suggest that this dissociative product originates mainly from subsequent dissociation of CF_2^+ formed by charge transfer. The precursor of the dissociative product CFD^+ is presumably CF_2D^+.

(5) A potential surface model based on transitions at crossings of potential energy surfaces of the dication-neutral system with coulomb repulsion surfaces of two singly charged products in the reactant (charge transfer) and product (chemical rearrangement) valley was described and applied to explain the competition of various processes in the studied system and in some other systems studied by others.

Acknowledgements

The authors gratefully acknowledge helpful discussions with I. Koyano, K. Inaoka, and S.D. Price and partial support of this research by grant no. 203/97/0351 of the Grant Agency of the Czech Republic and grant no. 440410 of the Grant Agency of the Academy of Science. One of the authors (Z.H.) wishes to express his thanks for the Alexander von Humboldt Research Award (1992) and for the hospitality of the Max-Planck Institut für Strömungsforschung in Göttingen (1993–1996), where early results of this study were evaluated.

References

[1] R.K. Janev, H. Winter, Phys. Rep. 117 (1985) 267.
[2] D. Mathur, Phys. Rep. 225 (1993) 193.
[3] Z. Herman, Int. Rev. Phys. Chem. 15 (1996) 299.
[4] A. Ehbrecht, N. Mustafa, Ch. Ottinger, Z. Herman, J. Chem. Phys. 105 (1996) 9833.
[5] K.G. Spears, F.C. Fehsenfeld, F. McFarland, E.E. Ferguson, J. Chem. Phys. 56 (1972) 2562.
[6] J.C. Weisshaar, Acc. Chem. Res. 26 (1993) 231.
[7] R. Tonkyn, J.C. Weisshaar, J. Am. Chem. Soc. 108 (1986) 7128.
[8] Y.A. Ranasighe, T.J. MacMahon, B.S. Freiser, J. Phys. Chem. 95 (1991) 7721.
[9] J.R. Gord, B.S. Fresier, S.W. Bruckner, J. Chem. Phys. 91 (1989) 7530.
[10] S.D. Price, M. Manning, S.R. Leone, J. Am. Chem. Soc. 116 (1994) 8673.
[11] Z. Dolejšek, M. Fárník, Z. Herman, Chem. Phys. Lett. 235 (1995) 99.
[12] K.A. Newson, S.D. Price, Chem. Phys. Lett. 269 (1997) 93.
[13] K.A. Newson, S.D. Price, Chem. Phys. Lett. 294 (1998) 223.
[14] B. Friedrich, Z. Herman, Coll. Czech Chem. Commun. 49 (1984) 570.
[15] S.G. Lias, J.E. Bartmess, J.F. Liebmann, J.L. Holmes, R.D. Levin, W.C. Mallard, J. Phys. Chem. Ref. Data 17 (1988) 9 (suppl. 1).
[16] J.M. Dyke, L. Golob, N. Jonathan, A. Morris, M. Okuda, J. Chem. Soc. Faraday Trans. 2, 70 (1974) 1828.
[17] J. Hrušák, N. Sändig, W. Koch, Z. Herman, Chem. Phys. Lett., in press.
[18] M. Manning, S.D. Price, S.R. Leone, J. Chem. Phys. 99 (1993) 8695.
[19] J. Žabka, Z. Herman, Czech J. Phys. 49 (1999) 373.
[20] A. Ehbrecht, N. Mustafa, Ch. Ottinger, Z. Herman, J. Chem. Phys. 105 (1996) 9833.
[21] M. Kimura, T. Iwai, Y. Kaneko, N. Kobayashi, A. Matsumoto, S. Ohtani, K. Okuno, S. Takaji, H. Tawara, S. Tsurubuchi, J. Phys. Soc. Jpn. 53 (1984) 2224.
[22] R.E. Olson, A. Salop, Phys. Rev. A 14 (1976) 579.
[23] D.K. Bohme, private communication.
[24] P. Tosi, R. Correale, W. Lu, S. Falcinelli, D. Basi, Phys. Rev. Lett. 82 (1999) 450.
[25] N. Sändig, W. Koch, J. Hrušák, private communication.
[26] B.P. Tsai, J.H.D. Eland, Int. J. Mass Spectrom. Ion Processes 36 (1980) 143.